West Chester University
Digital Commons @ West Chester University

Chemistry | College of Arts & Sciences

2011

Rational Design of Etchants For Electroless Porous Silicon Formation

Kurt Kolasinski
West Chester University, kkolasinski@wcupa.edu

J W. Gogola

Follow this and additional works at: http://digitalcommons.wcupa.edu/chem_facpub

Part of the Chemistry Commons

Recommended Citation
Kolasinski, K., & Gogola, J. W. (2011). Rational Design of Etchants For Electroless Porous Silicon Formation. *Pits and Pores 4: New Materials and Applications - in Memory of Ulrich Gosele, 33*(16), 23-28. http://dx.doi.org/10.1149/1.3553152

This Conference Proceeding is brought to you for free and open access by the College of Arts & Sciences at Digital Commons @ West Chester University. It has been accepted for inclusion in Chemistry by an authorized administrator of Digital Commons @ West Chester University. For more information, please contact wcressler@wcupa.edu.

Notice – Warning Concerning copyright Restrictions

The Copyright Law of the United States (Title 17, United States Code) governs the making of photocopies or other reproductions of copyrighted materials. Under certain conditions specified in the law, libraries and archives are authorized to furnish a photocopy or other reproduction. One of these specified conditions is that the photocopy or reproduction is not to be used for any purpose other than private study, scholarship, or research. If electronic transmission of reserve material is used for the purposes in excess of what constitutes "fair use," that user may be liable for copyright infringement. This institution reserves the right to refuse to accept a copying order if, in its judgment fulfillment of the order would involve violation of Copyright Law.

ECS Transactions, 33 (16) 23-28 (2011)
10.1149/1.3553152 ©The Electrochemical Society

Rational Design of Etchants for Electroless Porous Silicon Formation

Kurt W. Kolasinski and Jacob W. Gogola

Department of Chemistry, West Chester University, West Chester, PA 19383, USA

From fundamental considerations of the surface chemistry of Si etching in fluoride solutions as well as pore formation and propagation, we develop a mechanistic understanding of what must be known for rational development of etchants: (1) an acidic fluoride solution because the presence of OH^- promotes step flow etching, (2) sufficiently high fluoride concentration compared to the oxidant concentration, (3) the oxidant must be able to inject holes into the Si valance band at a sufficient rate, hence $E^\circ > -0.7$ V is required, (4) oxide formation needs to be slow or nonexistent so as to avoid the formation of a uniform oxide and associated electropolishing, (5) reduction of the oxidant must lead to soluble products, (6) film homogeneity is enhanced if the oxidant's half-reaction does not evolve gas, and finally (7) the net etching reaction has to be sufficiently anisotropic to support pore nucleation and propagation.

Introduction

Stain etching of silicon is an electroless process (1, 2) that results in the formation of a nanocrystalline porous silicon (por-Si) layer, which can exhibit visible photoluminescence. By far the most common stain etchant is composed of an aqueous mixture of nitric acid and hydrofluoric acid. This is somewhat unfortunate as the reduction of HNO_3(aq) is extremely complex and leads to the formation of various gaseous nitrogen oxides. The complexity and disadvantages of the nitric acid system have led to the conclusion that stain etching is irreproducible and capable of only producing inhomogeneous porous silicon layers that are less than 1 μm thick (3). In this report we show that a deeper understanding of the processes that lead to electroless porous silicon formation allow us to rationally develop etchants with vastly superior characteristics as compared to the HNO_3 + HF system.

Using the rules derived by Kolasinski (1, 4), we have developed (5-9) new formulations of stain etchants that utilize Fe^{3+}, VO_2^+ and Ce^{4+} as the oxidant. These new formulations get around many of the problems associated with common nitrate/nitrite based stain etchants. The new formulations need no "activation", exhibit short if any induction time, produce homogeneous films and are quite reproducible. Film thicknesses of 10–20 μm are easily obtained in as little as 60 min of etching (4).

The combination of infrared (FTIR) and cross section measurements yields complimentary information because FTIR interrogates both the chemical state of the surface and the surface area, while the cross section measures thickness. In HF+V_2O_5 solutions, Kolasinski et al. (6) have shown that rate of film growth depends strongly on the oxidant and fluoride concentration. Addition of ethanol greatly decreases the etch rate and changes the pore morphology from a mixture of {100} + {110} planes to

predominantly {100} planes (6). A plot of thickness vs. etch time in aqueous solutions evolves from a quadratic to a linear dependence. Kolasinski and Yadlovskiy developed a model in which pores with a uniform diameter nucleate randomly, initially grow rapidly before slowing to grow at a constant rate after saturation of the number of pores. The pore density increases linearly with time before saturation, causing a transition from a quadratic to a linear growth rate phase. This model simultaneously fits both the short time and long time behavior of the thickness and surface area for the V_2O_5 etchant. Here we show that the nonlinear behavior of the film growth rate in Fe^{3+} solutions also follows this model. In addition we make quantitative comparisons of the hole injection rate in V_2O_5 as compared to Fe^{3+} etchants.

Experimental

Formation of por-Si by stain etching has been studied with infrared spectroscopy (FTIR), photoluminescence (PL) and scanning electron microscopy (SEM). Si(100) (*p*-type prime grade, 14–22 Ω cm resistivity), V_2O_5 (Fisher certified grade), $FeCl_3{\cdot}6H_2O$ (Fisher purified), and HF (JT Baker 48–51% analytical grade) were used. All etchants were aqueous with no added alcohol or surfactant. Samples were rinsed in 1:1 water/ethanol then ethanol (three times), and dried in a stream of Ar. Scanning electron microscopy (SEM) was performed with an FEI Quanta 400 ESEM. Fourier transform infrared spectroscopy (FTIR) was performed with a Nicolet Protégé 460. IR spectra were recorded with a diffuse reflectance attachment purged with dry N_2 at a resolution of 4 cm^{-1} by averaging 512 scans. A planar hydrogen-terminated surface created by etching a polished Si(100) wafer in 50% HF for 5 min was used for a reference spectrum.

Results

Roughly 1 cm^2 substrates were etched in V_2O_5 + HF or $FeCl_3{\cdot}6H_2O$ + HF and the surface area and thickness were followed as a function of etch time. The results are shown in Fig. 1 below. Note that the integrated IR absorption peak area is plotted in these figures. As discussed previously [6], this peak area is proportional to the true surface area; however, we have not determined the proportionality constant to arrive at the absolute magnitude.

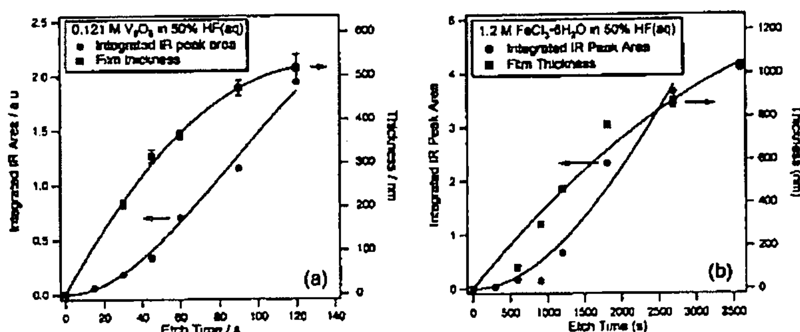

Figure 1 Thickness and integrated IR peak area versus time for porous films formed in (a) V_2O_5 + HF(aq) and (b) $FeCl_3{\cdot}6H_2O$ + HF(aq). The peak area is proportional to surface area.

Discussion

Kolasinski and Yadlovskiy have previously analyzed the increase in surface area and thickness of por-Si film formed in V_2O_5 + HF solutions (5). They developed a model similar to that of Brumhead et al. (10), who proposed that film formation begins when fast developing pores nucleate and propagate from the surface into the bulk. During the nonlinear growth rate phase, the number of pores increases until the density reaches a saturation value that achieves carrier depletion in the nanoscale-width pore walls. We model the porous layer as being composed of an array of cylinders oriented perpendicular to the exterior surface of the film. The thickness increases quadratically in time during the initial portion of film formation

$$h = k_0 t + k_1 t^2 \qquad [1]$$

as shown in Fig. 1. If the number of pores N increases linearly in time according to

$$N = k_2' t\,, \qquad [2]$$

then the surface area A of N cylinders in a film with thickness greater than their radius, $h \gg r$ is given by

$$A = \pi r\left(k_2' t\right)\left(k_0 t + k_1 t^2\right) = k_2 t\left(k_0 t + k_1 t^2\right). \qquad [3]$$

The constants k_0 and k_1 are determined uniquely from the h vs. t data and the constant k_2 is then determined independently from the FTIR data. The derivative of Eq. [1] yields the linear etch rate

$$R_h = dh/dt = k_0 + 2k_1 t\,. \qquad [4]$$

The constant k_0, therefore, is equal to the etch rate at time $t = 0$, which is not influenced by diffusion through the layer and represents a good quantity to quantitatively compare the efficacy of various oxidants at inducing por-Si formation. For the 0.121 M V_2O_5 solution we find that the initial etch rate is $R_{h,0} = 7.52 \pm 0.19$ nm s^{-1} and for the 1.2 M $FeCl_3{\cdot}6H_2O$ solution $R_{h,0} = 0.42 \pm 0.06$ nm s^{-1}.

Previously we have introduced the reactive sticking probability s_R as a measure of the efficiency of charge transfer between the Si and the oxidant (6). The reactive sticking coefficient is a measure of the probability that a collision of an oxidant with the surface leads to hole injection and then removal of a silicon atom. The etch rate is determined by the rate of hole injection (11, 12). Theoretically one Si atom is etched for each hole injected. In practice, many of the holes are lost to recombination or other nonetching related processes. The initial reactive sticking coefficient $s_{R,0}$ is given by the ratio of the number of atoms etched to the number of collision of the oxidant with the surface, and can be written as

$$s_{R,0} = \frac{R_{h,0}\,\rho_A\,\varepsilon}{n_t\,Z_w} = 7.923\times 10^{23}\,\frac{R_{h,0}\;\varepsilon M^{1/2}}{n_t\;c}, \qquad [5]$$

where the porosity is ε, ρ_A is the atomic density of Si, Z_w the collision frequency of the oxidant, n_t the number of holes transferred per collision, c the concentration in m^{-3} of the oxidant, and M its molar mass in g mol^{-1}. The porosity of our films is roughly 0.8 based on reflectometry measurements. For both reactions $n_t = 1$:

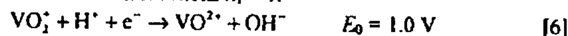

$$VO_2^+ + H^+ + e^- \rightarrow VO^{2+} + OH^- \qquad E_0 = 1.0\text{ V} \qquad [6]$$

$$Fe^{3+} + e^- \rightarrow Fe^{2+} \qquad E_0 = 0.77\text{ V}. \qquad [7]$$

For a 0.121 mol L^{-1} solution of V_2O_5 in 50% HF, assuming that all of the V_2O_5 dissolved to produce VO_2^+, the reactive charge transfer probability was $s_{R,0} = 3.0 \times 10^{-8}$. The reactive charge transfer probability is related to the charge transfer probability by

$$s_{R,0} = P_R\, i_e\,. \qquad [8]$$

where P_R is the survival probability of the hole, that is, one minus the probability that the hole is lost to nonetching related relaxation. The reactive charge transfer probability was very low either because very few holes are injected per collision of VO_2^+ with the surface and/or because the vast majority of the injected holes were lost to relaxation. For a 1.2 mol L^{-1} solution of Fe^{3+}, it is unclear what the solution phase species is. Most likely the Fe(III) is octahedrally coordinated in a complex of the form $[Fe(H_2O)_{6-n}Cl_n]^{3-n}$ with n = 0–3 (13). The uncertainty in the mass leads to some uncertainty in the reactive charge transfer probability, which can nonetheless be estimated as $s_{R,0} = 5 \times 10^{-10}$.

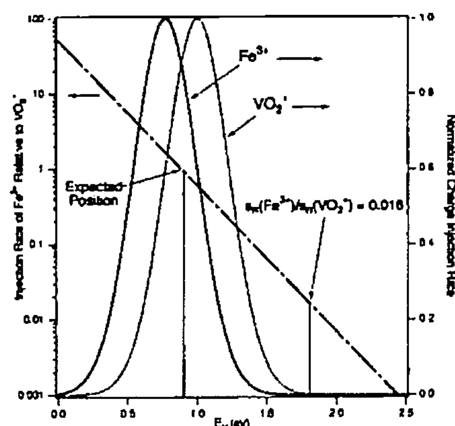

Figure 2. Calculated normalized rates of charge injection for Fe^{3+} and VO_2^+ (right axis) and the charge injection rate of Fe^{3+} relative to that of VO_2^+ (left axis).

The equilibrium charge transfer probability via the valence band is given by (14)

$$i_s = k_v^-\left(N_V - p_s^\circ\right)\exp\left[-\left(E_{ox}^\circ - E_V\right)^2/4\lambda k_B T\right]. \qquad [9]$$

where k_v^- a rate constant, N_V the density of states at the valence band edge, p_s° the concentration of holes at the surface, the reorganization energy λ, position of acceptor level E_{ox}°, position of the valence band maximum (VBM) E_V, absolute temperature T and k_B the Boltzmann constant must all be specified. The first three parameters should be independent of the oxidant in the solution because the surface is H-terminated in both cases and any effective doping changes caused by H^+ or F^- penetration into the depletion layer are not changed by the presence of the oxidant. Thus, the normalized hole injection rate depends only on the exponential term. Substituting $\lambda = 1$ eV and $T = 300$ K, the normalized hole injection rates for Fe^{3+} and VO_2^+ can be calculated. The results of this calculation are shown in Fig. 2 as a function of the energy of the valence band maximum. If $E_V = 0.9$ V, which is its position relative to the standard hydrogen electrode in 5 M HF (15), then on the basis of this calculation we would expect $s_{R,0}(\text{Fe(III)})/s_{R,0}(\text{V(V)}) = 0.94$ assuming that P_R is the same in both instance. Since both Fe(III) and V(V) transfer holes into the surface through one-electron transfers, it seems likely that P_R should be approximately the same in both cases. However, the measured

value of $s_{R,0}(\text{Fe(III)})/s_{R,0}(\text{V(V)}) = 0.016$. Therefore, either the valence band maximum has been shifted to $E_V = 1.81$ V (see Fig. 2) or else the rate at which holes are injected by Fe(III) is much lower than expected based on the Marcus theory expression in Eq. [9]. To help us answer this question we need to measure $s_{R,0}$ for at least one other species. We have already demonstrated that Ce(IV) effectively produces por-Si (7, 16). We have also found that HIO_3 etches Si in HF(aq) but that por-Si formation is hampered by precipitation.

Si atoms are removed according to the Gerischer mechanism (11, 17, 18). Conclusive evidence against formation of SiO_2 (or suboxide) and chemical removal by HF is obtained by examination of bubble formation (5). In any mechanism of stain etching, such as the Turner mechanism, that involves an oxide intermediate the formation of bubbles can only result from reactions involving the oxidant. For example, when HNO_3 is used as an oxidant various reductions result in the production of NO_x. All of the gas should be NO_x and not H_2. However, Kooij et al. (19) found that H_2 is formed in a 4:1 ratio compared to NO_x. On the other hand, in the Gerischer mechanism H_2 is formed from hydrolysis of an etch product and the counter reaction required for charge balance. These reactions need not occur where etching occurs; therefore, bubbles can form remotely, either in solution or on other parts of the crystal. This is exactly what we observed. Initially bubbles form on the edges of the crystal and along scratches in the surface. Unlike metals, Si is a poor catalyst for H_2 production and; therefore, the bubbles form first and primarily at highly defective regions of the crystal.

Conclusion

Rational formulation of stain etchants to produce films of nanocrystalline porous silicon is possible once the dynamics of porous film formation are understood (4). The guidelines for formulation are (i) an acidic fluoride solution because the presence of OH^- promotes step flow etching, (ii) sufficiently high fluoride concentration compared to the oxidant concentration, (iii) the oxidant must be able to inject holes into the Si valance band at a sufficient rate, hence $E^\circ > -0.7$ V is required, (iv) oxide formation needs to be slow or nonexistent so as to avoid the formation of a uniform oxide and associated electropolishing, (v) reduction of the oxidant must lead to soluble products, (vi) film homogeneity is enhanced if the oxidant's half-reaction does not evolve gas, and finally (vii) the net etching reaction has to be sufficiently anisotropic to support pore nucleation and propagation. Here we report the first quantitative comparison of the efficacy of two different oxidants at inducing porous silicon formation. We find that the reactive charge transfer probability is $s_{R,0} = 3 \times 10^{-8}$ for VO_2^+ and $s_{R,0} = 5 \times 10^{-10}$ for Fe(III). Further experiments are underway to determine whether the difference in efficacy can be ascribed to the dependence of the hole injection rate on the position of the valence band maximum or to significantly different hole survival probabilities subsequent to injection.

Acknowledgments

Supported by West Chester University, the Pennsylvania State System of Higher Education, the Center for Microanalysis and Imaging, Research and Training (CMIRT) at WCU and the expert technical assistance of Frederick Monson.

References

1. K. W. Kolasinski, New Approaches to the Production of Porous Silicon by Stain Etching. In *Nanostructured Semiconductors: from basic research to applications*, P. Granitzer and K. Rumpf, Eds., in press, Pan Stanford Publishing, Singapore (2011).
2. K. W. Kolasinski, *Curr. Opin. Solid State Mater. Sci.*, **9** (1-2), 73 (2005).
3. V. Lehmann, *Electrochemistry of Silicon: Instrumentation, Science, Materials and Applications*, Wiley-VCH, Weinheim (2002).
4. K. W. Kolasinski, *J. Phys. Chem. C*, (accepted) (2010).
5. K. W. Kolasinski and J. Yadlovskiy, *Phys. Status Solidi C*, (accepted) (2010).
6. K. W. Kolasinski, J. D. Hartline, B. T. Kelly and J. Yadlovskiy, *Mol. Phys.*, **108** (7), 1033 (2010).
7. M. E. Dudley and K. W. Kolasinski, *Electrochem. Solid State Lett.*, **12** (4), D22 (2009).
8. M. E. Dudley and K. W. Kolasinski, *Phys. Status Solidi A*, **206** (6), 1240 (2009).
9. M. Nahidi and K. W. Kolasinski, *J. Electrochem. Soc.*, **153** (1), C19 (2006).
10. D. Brumhead, L. T. Canham, D. M. Seekings and P. J. Tufton, *Electrochim. Acta*, **38** (2/3), 191 (1993).
11. H. Gerischer, P. Allongue and V. Costa Kieling, *Ber. Bunsen-Ges. Phys. Chem.*, **97** (6), 753 (1993).
12. H. Gerischer and F. Beck, *Z. Phys. Chem. (Neue Folge)*, **24**, 378 (1960).
13. M. Magini and T. Radnai, *J. Chem. Phys.*, **71** (11), 4255 (1979).
14. H. Gerischer, Principles of Electrochemistry. In *The CRC Handbook of Solid State Electrochemistry*, P. Gellings and H. Bouwmeester, Eds., pp 9-72, CRC Press, Boca Raton (1997).
15. P. Gorostiza, P. Allongue, R. Diaz, J. R. Morante and F. Sanz, *J. Phys. Chem. B*, **107** (26), 6454 (2003).
16. M. E. Dudley and K. W. Kolasinski, *ECS Trans.*, **16** (3), 323 (2008).
17. K. W. Kolasinski, *Phys. Chem. Chem. Phys.*, **5** (6), 1270 (2003).
18. K. W. Kolasinski, *Surf. Sci.*, **603** (10-12), 1904 (2009).
19. E. S. Kooij, K. Butter and J. J. Kelly, *Electrochem. Solid State Lett.*, **2** (4), 178 (1999).